Solar-Terrestrial Physics, 2018. Vol. 4. Iss. 2, pp. 41–48, DOI: 10.12737/stp-42201807. © 2018 V.N. Gubenko, I.A. Kirillovich. Published by INFRA-M Academic Publishing House
Original Russian version: V.N. Gubenko, I.A. Kirillovich, published in Solnechno-zemnaya fizika, 2018, vol. 4, iss. 2, pp. 76–85, DOI: 10.12737/szf-42201807 © 2018 INFRA-M Academic Publishing House (Nauchno-Izdatelskii Tsentr INFRA-M)

DIAGNOSTICS OF INTERNAL ATMOSPHERIC WAVE SATURATION AND DETERMINATION OF THEIR CHARACTERISTICS IN EARTH'S STRATOSPHERE FROM RADIOSONDE MEASUREMENTS

V.N. Gubenko
Kotel'nikov Institute of Radio Engineering and Electronics RAS, Fryazino, Russia, vngubenko@gmail.com

I.A. Kirillovich
Kotel'nikov Institute of Radio Engineering and Electronics RAS, Fryazino, Russia, sabersecretmail@gmail.com

Abstract. Internal gravity waves (IGW) significantly affect the structure and circulation of Earth's atmosphere by transporting wave energy and momentum upward from the lower atmosphere. Since IGW can propagate freely through a stably stratified atmosphere, similar effects may occur in the atmospheres of Mars and Venus. Observations of temperature and wind speed fluctuations induced by internal waves in Earth's atmosphere have shown that wave amplitudes increase with height, but not quickly enough to correspond to the amplitude increase due to an exponential decrease in the density without energy dissipation. The linear theory of IGW explains the wave amplitude growth rate as follows: any wave amplitude exceeding the threshold value leads to instability and produces turbulence, which hinders further amplitude growth (internal wave saturation). The mechanisms that contribute most to the energy dissipation and saturation of IGW in the atmosphere are thought to be the dynamical (shear) and convective instabilities. The assumption of internal wave saturation plays a key role in radio occultation monitoring of IGW in planetary atmospheres. A radiosonde study of wave saturation processes in Earth's atmosphere is therefore actual and important task. We report the results of determination of actual and threshold amplitudes, saturation degree, and other characteristics for the identified IGW in Earth's atmosphere obtained from the analysis of SPARC (Stratospheric Processes And their Role in Climate) radiosonde measurements of wind speed and temperature [http://www.sparc.sunysb.edu/].

Keywords: Earth's atmosphere, internal gravity waves, saturation, radiosonde measurements, wind speed, temperature.

INTRODUCTION

The principal objective of planetary atmosphere physics is to study wave processes that, as shown by observations, determine the atmospheric dynamics at all heights [Gubenko et al., 2012]. A key role of internal gravity waves (IGW) is primarily connected with the fact that they provide an effective mechanism for energy and momentum transfer upward from the lower atmosphere. Ionosphere experts evince great interest in IGW because many ionospheric and radio wave propagation processes are well explained through atmospheric waves. According to the currently adopted interpretation, traveling ionospheric disturbances and sporadic E_s-layers are ionospheric manifestations of waves in an essentially neutral atmosphere [Gossard, Hooke, 1978; Gubenko et al., 2018]. Generation sources of IGW in the atmosphere may be near-surface thermal contrasts, topography, wind shear instability, convection, and frontal processes. In Earth's atmosphere in the absence of energy dissipation, the amplitude of wave disturbances of wind speed or temperature increases approximately exponentially with height. Near-surface low-amplitude disturbances can therefore produce significant effects at large heights, where waves break down and the IGW energy and momentum are transferred to the undisturbed flow. Since IGW represent a characteristic feature of a stably stratified atmosphere, similar effects can occur in the atmospheres of Venus and Mars. Internal waves in the Martian atmosphere are thought to play a more important role than those in Earth's atmosphere because in many cases the IGW amplitudes in the Martian atmosphere are much higher than their terrestrial counterparts [Creasey et al., 2006; Gubenko et al., 2008a, 2012, 2015, 2016a].

Studying internal waves with any techniques faces a problem, the core of which is that the disturbed atmosphere parameters such as wind speed, temperature, or density are measured; and this measurement is to be used to determine which part of the "signal" is induced by IGW. The general approach here is to separate small-scale variations from slow changes in undisturbed background and consider these variations to be related to wave processes. So, if the measurements are time realizations for a fixed observation point, such as lidar or radar measurements, the above separation of scales can be effected through a frequency analysis. Approaches using any separations of scales must take into account that not all small-scale atmospheric variations are caused by IGW. The observed variations may also be associated with the influence of regular thin layers or turbulence in a planetary atmosphere. To interpret the measurements correctly, we should have a discrimination criterion for identifying wave events. Only when this criterion is met, the analyzed variations can be considered as manifestations of waves in a planetary at-

mosphere [Gubenko et al., 2008b, 2011, 2012, 2015, 2016a, b, c].

Radio occultation satellite observations in the atmosphere are an effective tool of radio physical research into IGW activity throughout the planet based on nearly uniform and high-quality experimental data [Gorbunov, Gurvich, 1998]. The analysis of vertical temperature variation profiles determined from radio occultation experiments has revealed some statistical characteristics (potential energy of IGW per unit mass) of internal waves in Earth's atmosphere [Steiner, Kirchengast, 2000; Tsuda et al,. 2000; Tsuda, Hocke, 2002]. An advantage of radio occultation measurements in studying internal atmospheric waves is a wider geographical and temporal coverage of areas of interest, which enables global monitoring of wave activity in a planetary atmosphere [Gavrilov et al., 2004; Gavrilov, Manuilova, 2016]. This method allows us to obtain vertical profiles of atmospheric parameters (pressure, density, and temperature) at a global scale with high vertical resolution in any weather conditions [Liou et al., 2003, 2004; Pavelyev et al., 2009, 2012, 2015]. However, until recently, researchers believed that the reconstructed vertical temperature and density profiles in radio occultation experiments are not enough to quantify the wave effects in a planetary atmosphere [Gubenko et al., 2012, 2015].

In this regard, we have developed an original method of identifying discrete wave events and reconstructing IGW parameters from an analysis of the individual vertical temperature, density, or squared Brunt–Väisälä frequency profile in a planetary atmosphere [Gubenko et al., 2008b, 2011, 2012, 2015]. The method does not require any additional information not contained in the profile and can be adopted to analyze vertical profiles obtained by various methods. We have formulated and justified a threshold criterion for identifying wave events; its fulfillment assumes the analyzed variations to be manifestations of waves [Gubenko et al., 2008b, 2011, 2012, 2015, 2016b]. The method relies on the analysis of the relative wave amplitude, determined from the vertical profile of temperature or density, as well as on the concept of the linear IGW theory, which suggests that the wave amplitude is limited by threshold values due to dynamic (shear) instability in the atmosphere. It is expected that when the internal wave amplitude reaches the shear instability threshold as the wave propagates upward, wave energy dissipation occurs so that the IGW amplitude stays at the atmospheric instability threshold (wave amplitude saturation). To test this method, we have used simultaneous probe measurements of temperature and wind speed in Earth's stratosphere [Cot, Barat, 1986]. By analyzing the wind speed hodograph, Cot and Barat [1986] identified the saturated IGW and determined its characteristics. The probe temperature measurements and the method we developed allowed us to independently reconstruct all characteristics of the identified internal wave with errors not exceeding 30 % [Gubenko et al., 2008b, 2012]. The application of the method to the analysis of radio occultation temperature data enabled us for the first time to identify wave events in the atmospheres of Earth and Mars, to determine the key characteristics of the detected waves, including intrinsic frequency of IGW, vertical fluxes of wave energy and momentum [Gubenko et al., 2008b, 2011, 2015, 2016a, b, c]. Results of wave activity monitoring can be useful in constructing numerical atmospheric circulation models involving parameterization of wave effects. Experimental determination and analysis of geographical and seasonal distributions of internal wave characteristics [Gubenko et al., 2012, 2015, 2016b] are necessary and important stages in developing adequate models of the general circulation in Earth's atmosphere. The original method of identifying wave events and reconstructing IGW characteristics in planetary atmospheres we developed [Gubenko et al., 2008b, 2011, 2012, 2015, 2016a, b, c] has been widely recognized by scientific community both in Russia and abroad. It is now being successfully used to study wave processes in the atmospheres of Earth [Horinouchi, Tsuda, 2009; Xiao, Hu, 2010; Rechou et al., 2014; Sacha et al., 2014; Noersomadi, Tsuda, 2017; Zagar et al., 2017] and Venus [Altieri et al., 2014; Peralta et al., 2015]. For example, Rechou et al. [2014] have shown that numerical simulation data and analysis of independent radar and probe measurements in Earth's atmosphere demonstrate high efficiency of our method and high reliability of scientific results it yields.

Radio occultation studies of internal waves in Earth's middle atmosphere [Gubenko et al. 2008b, 2011, 2012, 2016b] use data from one observation system. It generally provides information only about one independent variable (temperature or density) and leads to some ambiguity in the wave field description. Two instrumentation systems applied at a time enable a more complete characterization of the wave field and the IGW atmospheric effects. Simultaneous data on wind speed and temperature, derived from radiosonde measurements, allow us to pay more attention to the role played by internal waves in the atmospheric dynamics. In some respects, probe data make it possible to verify radio occultation wave studies, which rely on the analysis of the IGW-induced temperature or density variations under the saturated wave assumption (our SWA method). By measuring simultaneously temperature and wind speed disturbances and analyzing them, we can estimate the degree of the IGW saturation without any assumptions, assess the validity of the internal wave saturation assumption, and, therefore, determine the effectiveness of the SWA method. It is necessary to know the actual and threshold wave amplitudes to evaluate the influence of internal waves on the undisturbed atmosphere. Since the internal wave saturation assumption plays a key role in radiophysical monitoring of IGW in planetary atmospheres [Gubenko et al., 2008b, 2011, 2012, 2015, 2016a, b, c], radiosonde studies of saturation processes in Earth's atmosphere are relevant and important. To radiosonde studies of IGW we apply the classical method of wind speed hodograph analysis. The advanced hodograph method we propose relies on a

combined analysis of simultaneous measurements of wind speed and temperature, which uses a polarization relation between wave variations of speed and temperature to realize minimum errors in results of reconstruction of internal atmospheric wave characteristics.

THEORETICAL RELATIONS AND HODOGRAPH METHOD

The dispersion equation relates the intrinsic wave frequency ω (frequency determined in the reference system that moves with an undisturbed wind speed) to the IGW spatial characteristics (horizontal k_h and vertical m wavenumbers) and to the stability parameter of undisturbed atmospheric stratification N_b (buoyancy (Brunt–Väisälä) frequency). If hydrostatic regime conditions hold for internal waves: $N_b^2 >> \omega^2 > f^2$, $m^2 >> k_h^2$, and $m^2 >> (2H)^{-2}$, the dispersion equation takes the form [Fritts, Alexander, 2003; Gubenko et al., 2008b, 2011, 2012]:

$$(c-\bar{u})^2 = \frac{\omega^2}{k_h^2} = \frac{N_b^2}{m^2}\frac{1}{1-f^2/\omega^2}, \quad (1)$$

where $(c-\bar{u})$ is the intrinsic horizontal phase speed, c is the ground-based horizontal phase speed (fixed reference system), $\bar{u}$ is the projection of undisturbed wind speed on direction of vector $\mathbf{k}_h$ and $H \simeq 7$ km is the scale height of Earth's middle atmosphere. Inertial frequency (Coriolis parameter) f is given by $f=2\Omega\sin\varphi$, where $\Omega=7.292\cdot10^{-5}$ rad/s is Earth's rotation rate and φ is the latitude. The vector (k_h, m) determines the wave phase propagation direction. For internal waves whose energy is transferred upward (upward group speed component), the phase is downward (m<0), and vice versa. The intrinsic frequency is considered to be positively defined (ω>0).

If an axis of the coordinate system is selected in the direction of the horizontal wave vector component $\mathbf{k}_h$, the polarization relations take a simple form [Zink, Vincent, 2001; Gubenko et al., 2008b, 2011, 2012]:

$$v' = -i\frac{f}{\omega}u', \quad (2)$$

$$w' = -\frac{k_h}{m}u', \quad (3)$$

$$u' = i\frac{g}{N_b}\frac{\hat{T}'}{\sqrt{1-f^2/\omega^2}}, \quad (4)$$

where u' and v' are the complex disturbances of wind speed components directed parallel and perpendicular to the horizontal wave vector component respectively; w' is the complex disturbance of wind speed in the vertical direction; $\hat{T}' = T'/T_b$ is the normalized complex disturbance of absolute temperature (T=t+273°); i is the imaginary unit. Complex and real physical disturbances are connected by simple relations. For example, to the complex disturbance u' corresponds the real disturbance Re u', and its amplitude is equal to $|u'|$ [Gubenko et al., 2008b, 2012]. From Equation (2) it follows that the phase difference between u' and v' disturbances is 90°, and the amplitude ratio $|v'|/|u'|$ is equal to f/ω. Since the horizontal wind speed hodograph describes an ellipse and the motion occurs in a plane perpendicular to the wave vector [Gill, 1986], a low-frequency IGW at $\omega\sim f$ is an elliptically polarized transverse wave. At higher frequencies when the inequality $f/\omega \ll 1$ is valid, the ellipse transforms into a straight line and internal waves become linearly polarized. Note that polarization relation (4) holds for internal waves whose energy is transferred upward (m<0), otherwise (m>0) we should change sign from plus to minus in the right hand side of Equation (4) [Pfister et al., 1993]. Dispersion equation (1) and polarization relations (2)–(4) are approximations for which there are two intervals in the hydrostatic wave regime. Range of intermediate intrinsic frequencies is defined as the range of frequencies ω such that $N_b^2 >> \omega^2 >> f^2$. Dispersion equation (1) here becomes much simpler and yields a simple connection of the intrinsic horizontal phase speed $(c-\bar{u})$ with the vertical wavenumber m and Brunt–Väisälä frequency: $|c-\bar{u}| = \omega/|k_h| = N_b/|m|$ [Fritts, Alexander, 2003; Gubenko et al., 2012]. Range of low intrinsic frequencies is defined as the range of frequencies such that ω^2 has the same order as f^2, but $\omega^2 > f^2$.

To calculate the buoyancy frequency N_b from measurements of the vertical temperature profile $T_b(z)$, we use the following expression [Gubenko et al., 2008b, 2011, 2012]:

$$N_b^2 = \frac{g}{T_b}\left(\frac{\partial T_b}{\partial z} + \frac{g}{c_p}\right), \quad (5)$$

where g is the free fall acceleration, $g/c_p=9.8\cdot10^{-3}$ K/m is the adiabatic temperature gradient, T_b is the undisturbed (mean) absolute temperature, z is the local vertical coordinate.

The idea of the hodograph analysis involves monitoring the motion (rotation) of the vector of wind speed disturbances with height [Hines, 1988]. According to the theory, the wave hodograph (the trajectory described by the endpoint of the speed disturbance vector) is an ellipse whose major axis is parallel to the horizontal wave propagation direction, and lengths of the major and minor semi-axes of the ellipse are amplitudes of wind speed disturbances along the vector $\mathbf{k}_h$ and in a transverse direction respectively. The intrinsic wave frequency ω can be determined from the expression for the axial ratio AXR, which accounts for the effect of vertical shear of the transverse component of the mean wind speed V_T [Hines, 1988]:

$$AXR = \frac{|v'|}{|u'|} = \left|\frac{f}{\omega} - \frac{1}{N_b}\frac{dV_T}{dz}\right|, \quad (6)$$

where $|u'|$ and $|v'|$ are the lengths of the major and minor semi-axes of the ellipse respectively. Thus, by determining N_b, f/ω, ω, and $|m|=2\pi/\lambda_z$ (λ_z is the vertical wavelength) from the experiment and taking into account dispersion equation (1), we can find $|k_h|$, horizontal wavelength $\lambda_h=2\pi/|k_h|$, and intrinsic horizontal phase

speed $|c-\bar{u}|$. The amplitude of vertical speed disturbances $|w'|$ is determined from polarization relation (3).

To study the IGW saturation, we calculate the relative threshold amplitude a of shear instability using the ratio f/ω [Fritts, 1989]:

$$a=\frac{|u'_{\rm sat}|}{|c-\bar{u}|}-\frac{2\sqrt{1-f^2/\omega^2}}{1+\sqrt{1-f^2/\omega^2}}, \qquad (7)$$

where $|u'_{\rm sat}|$ is the amplitude of saturation for horizontal wind speed disturbances parallel to the vector $\mathbf{k}_{\rm h}$. The analysis of a particular radiosonde measurement session has provided us with two independent estimates of the relative wave amplitude $a_{\rm e}$ and $a_{\rm u}$ [Gubenko et al., 2011]:

$$a_{\rm e}=\frac{|u'|}{|c-\bar{u}|}=\frac{g|m|}{N_{\rm b}^2}|\hat{T}'|=\frac{2\pi g}{\lambda_z N_{\rm b}^2}|\hat{T}'|,$$

$$a_{\rm u}=\frac{|u'|}{|c-\bar{u}|}=\frac{|u'||m|}{N_{\rm b}}\sqrt{1-\frac{f^2}{\omega^2}}. \qquad (8)$$

The $a_{\rm e}$ value is calculated by analyzing only temperature data, whereas $a_{\rm u}$ is determined from measurements of both speed and temperature. We interpret the IGW saturation degree as the ratio of the speed disturbance amplitude $|u'|$ to the saturated wave amplitude $|u'_{\rm sat}|$, and it can be found from expressions (8) in two different ways [Gubenko et al., 2011]:

$$d_{\rm e}=\frac{|u'|}{|u'_{\rm sat}|}=\frac{a_{\rm e}}{a},$$

$$d_{\rm u}=\frac{|u'|}{|u'_{\rm sat}|}=\frac{a_{\rm u}}{a}. \qquad (9)$$

EXPERIMENTAL DATA AND DISCUSSION OF RESULTS

To demonstrate the possibilities of the method, we consider an example of its practical application to the analysis of simultaneous balloon measurements of temperature and wind speed in Earth's atmosphere. These measurements are freely available on the website of the SPARC Data Center [http://www.sparc.sunysb.edu/]. The measurements were recorded each 6 s. This corresponds to the ~30 m vertical resolution of data with the ~5 m/s mean rate of balloon rise. Accuracy of the temperature and wind speed measurements is ~0.2 K and 1 m/s respectively.

Figure 1 shows two temperature profiles derived from measurements in Earth's atmosphere over Desert Rock, which were made ~12 hrs apart. The vertical correlation of quasiperiodic temperature variations for these profiles in the given interval suggests that these variations may be generated by an IGW or by semidiurnal thermal tide with a period of ~12 hrs in the ground-based reference system. To test this hypothesis, we make a joint analysis of temperature data (Figure 1, left), zonal and meridional wind speeds (Figure 1, right) for the November 06, 2008 measurement session. For the zonal direction we take the west-east direction; for the meridional direction, the south-north one.

Figure 2 presents the analyzed profiles for the selected interval 22.5–30 km of wave manifestations. The dashed line shows the corresponding mean (undisturbed) profiles calculated by approximating the original data by the third-degree polynomial using a least squares method (LSM). By applying expression (5) to the mean temperature profile, we can estimate the Brunt–Väisälä frequency $N_{\rm b}$ (stability parameter of atmospheric stratification) $N_{\rm b}\simeq 2.18\cdot10^{-2}$ rad/s for the interval of interest.

Figure 3 depicts vertical profiles of temperature variations and speed components, which are defined as the difference between original and respective mean profiles in Figure 2. From these profiles we determine the amplitude of temperature variations $|T'|\simeq$ 2.74 K and the vertical wavelength $\lambda_z\simeq$ 3.4 km for the speed and temperature disturbances. We also choose the interval to plot the hodograph and determine the value $T_{\rm b}$ of the mean temperature $T_{\rm b}\simeq$ 218 K in the center of the specified interval at 26 km.

Figure 4 presents the hodograph of horizontal wind speed variations for a height interval 24.3–27.8 km. The abscissa and ordinate show values of zonal and meridional components respectively. Dots are original data, ⊙ is the initial point of hodograph; numbers near experimental points indicate height in kilometers. The arrow denotes the direction of the mean wind speed $\mathbf{V}_{\rm b}$ at 26 km. The smooth solid line shows the ellipse of the LSM approximation of the data under study, the lengths of the major and minor semi-axes of which determine the amplitudes $|u'|$ and $|v'|$ of horizontal speed disturbances: $|u'|\simeq$ 5.63 m/s and $|v'|\simeq$ 2.98 m/s. According to the IGW theory, the clockwise rotation of the vector endpoint of speed variations with increasing height in the Northern Hemisphere corresponds to downward phase propagation and upward transfer of wave energy.

We calculate the Coriolis parameter $f\simeq 0.86\cdot10^{-4}$ rad/s at the observation point and, using (6), find the f/ω ratio and the intrinsic frequency ω: $f/\omega\simeq$ 0.53 and $\omega\simeq 1.63\cdot10^{-4}$ rad/s (the intrinsic period of wave $T^{\rm in}=2\pi/\omega\simeq$ 10.7 hrs). Next, from Equation (1) we determine the intrinsic horizontal phase speed $|c-\bar{u}|\simeq$13.9 m/s and horizontal wavelength $\lambda_{\rm h}=|c-\bar{u}|T^{\rm in}\simeq$ 535 km. Taking into account relation (3), we find the amplitude of vertical wind speed disturbances $|w'|\simeq 3.6\cdot10^{-2}$ m/s. Using the known relation between the intrinsic frequency ω and the wave frequency σ in the ground-based reference system $\sigma=\omega+\mathbf{k_h}\mathbf{V_b}$, we determine σ. Knowing the direction of the major axis of the hodograph ellipse, we can find the horizontal direction of the wave vector $\mathbf{k}_{\rm h}$ with an uncertainty of 180°. The angle between $\mathbf{k}_{\rm h}$ and $\mathbf{V}_{\rm b}$ (Figure 4) is close to the right angle (92.2° or 87.8°), therefore $\mathbf{k}_{\rm h}\mathbf{V}_{\rm b}\simeq 0$ and $\sigma\simeq\omega\simeq 1.63\cdot10^{-4}$ rad/s. The wave period in the fixed reference system $T^{\rm ob}=2\pi/\sigma\simeq$10.7 hrs coincides with the intrinsic period $T^{\rm in}$, its value is close to the previously discussed value of ~12 hrs.

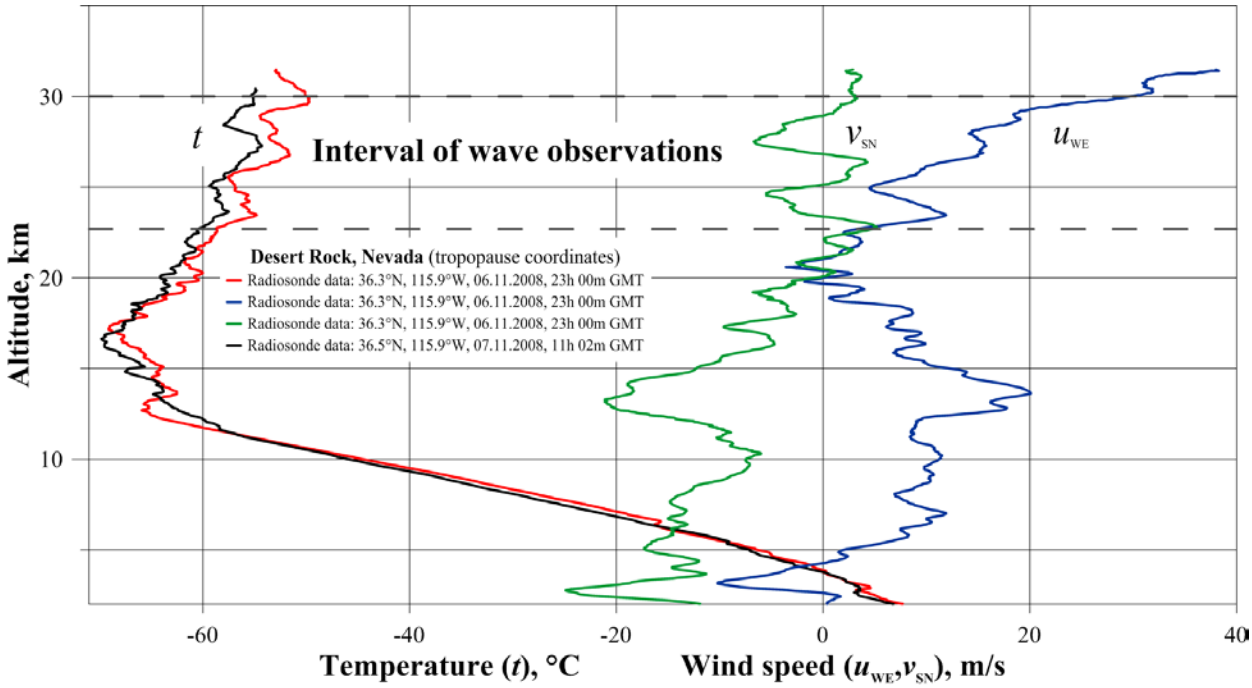

Figure 1. Vertical profiles of temperature *t*, zonal u_{WE} and meridional v_{SN} wind speed as derived from radiosonde measurements in the atmosphere over Desert Rock, Nevada

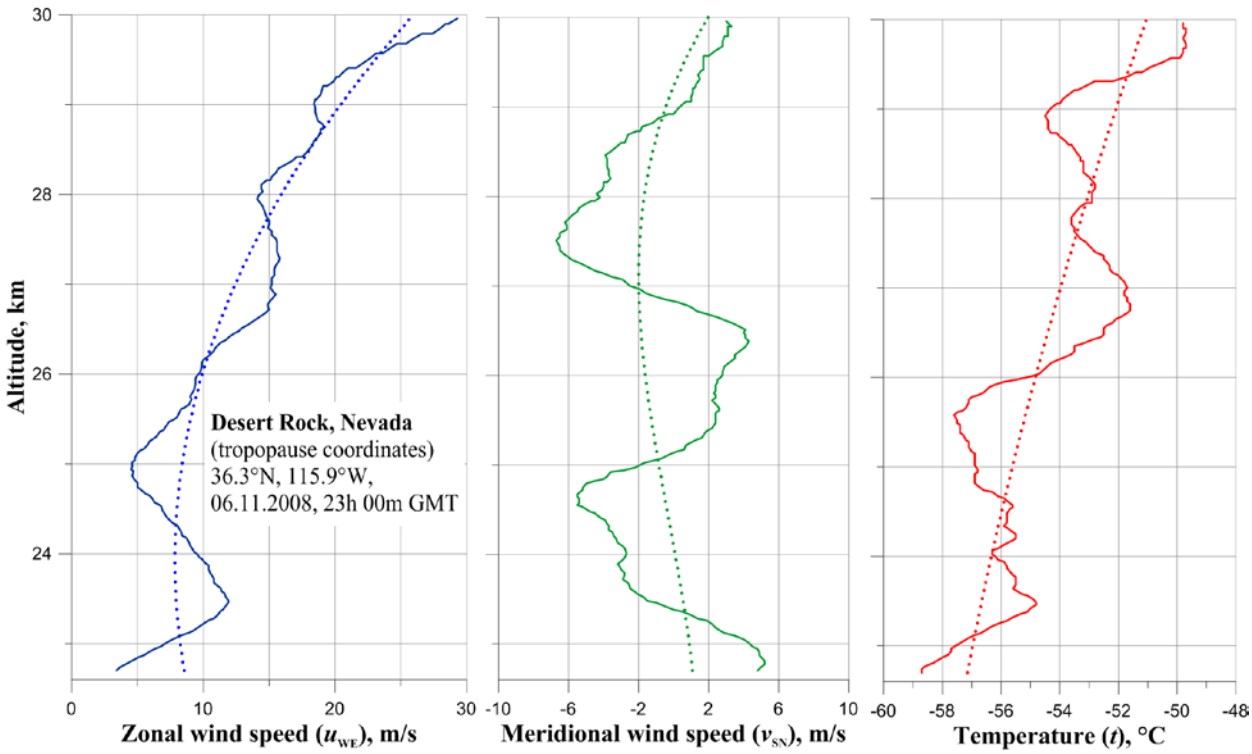

Figure 2. Vertical profiles of temperature, zonal and meridional wind speed components derived from probe measurements in the atmosphere over Desert Rock on November 06, 2008

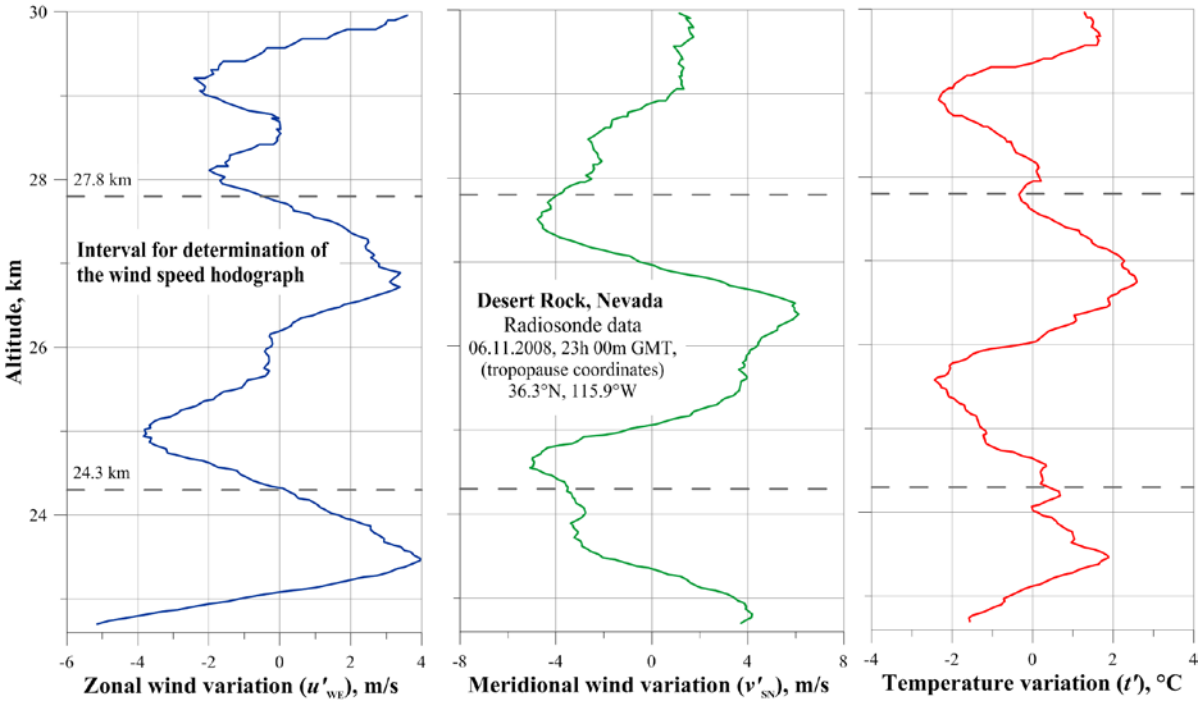

Figure 3. Vertical profiles of variations in temperature and wind speed components derived from radiosonde measurements in the atmosphere over Desert Rock on November 06, 2008

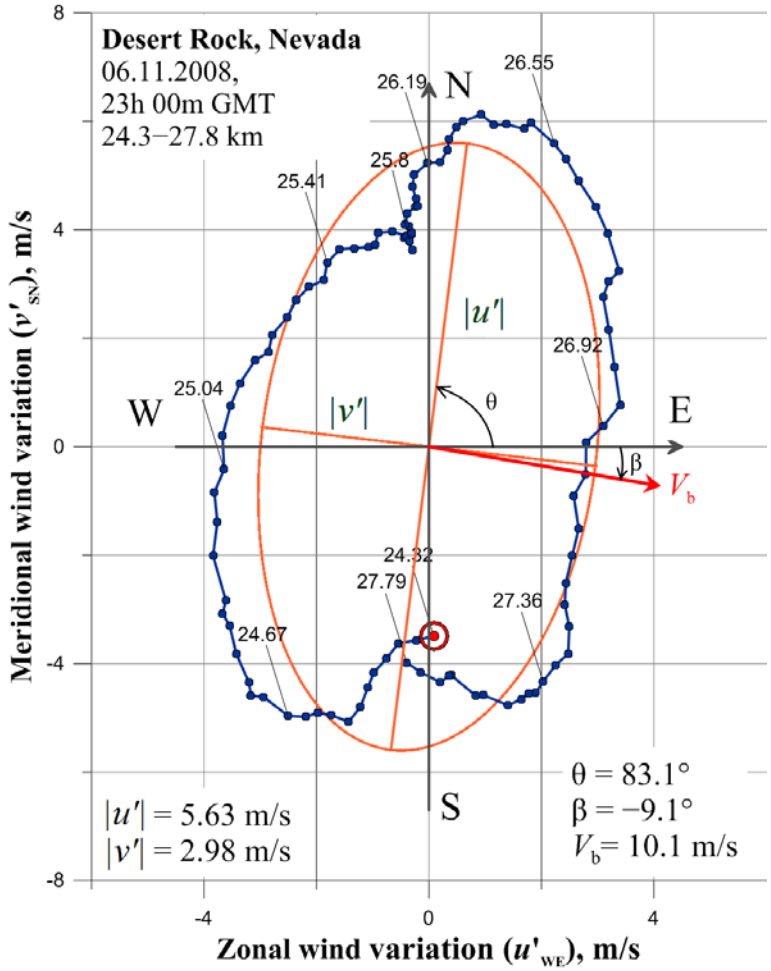

Figure 4. Hodograph of wind speed variations plotted for a height interval of 24.3 to 27.8 km

This supports the hypothesis that the observed quasi-periodic variations (Figure 1) are induced by the IGW, not by semidiurnal thermal tide.

Internal waves affect the undisturbed wind or lead to a mixing of atmospheric components only in case of wave energy dissipation. Dynamic and convective instabilities are believed to be the main processes leading to dissipation [Fritts, 1989; Fritts, Alexander, 2003], although there are other mechanisms (molecular diffusion, radiative damping, nonlinear interactions). Convective or dynamic instability causes an IGW to break when its amplitude exceeds a certain threshold. From expression (7) we calculate the threshold amplitude $a \simeq 0.92$ for the shear instability, which is essential for low-frequency IGW with $\omega \sim f$ [Fritts, 1989]. Due to the existence of threshold amplitudes, saturation mechanisms become non-linear, so it is important to know actual wave amplitudes in experiments. Expressions (8) yield two independent estimates of the wave amplitude $a_e \simeq 0.43$ and $a_u \simeq 0.40$, which agree well with each other. This indicates that the temperature and wind speed data are of high quality, and suggests that polarization relation (4) holds. From expressions (9) in two different ways, we evaluate the IGW saturation degree $d_e \simeq 0.47 = 47$ % and $d_u \simeq 0.44 = 44$ %.

The analysis shows that the proposed method allows us to reliably identify the IGW signatures in radiosonde measurements, and to determine characteristics and the saturation degree of internal waves in Earth's atmosphere without any assumptions. For radio occultation monitoring of wave activity in planetary atmospheres [Gubenko et al., 2008b, 2011, 2012, 2015], we use the saturated wave assumption. The results indicate that this assumption does not always hold, thus leading to systematic errors and aliasing of reconstructed wave characteristics. In particular, the intrinsic frequency can be systematically underestimated; and the horizontal wavelength, overestimated.

This work was partially supported by RAS Presidium Program 28. We thank two anonymous reviewers of the article for informative and constructive comments.

REFERENCES

Altieri F., Migliorini A., Zasova L., Shakun A., Piccioni G., Bellucci G. Modeling VIRTIS/VEX O2(a1Δg) nightglow profiles affected by the propagation of gravity waves in the Venus upper mesosphere. *J. Geophys. Res.* 2014, vol. 119, pp. 2300–2316. DOI: 10.1002/2013JE004585.

Cot C., Barat J. Wave-turbulence interaction in the stratosphere: A case study. *J. Geophys. Res.* 1986, vol. 91, no. D2, pp. 2749–2756.

Creasey J.E., Forbes J.M., Hinson D.P. Global and seasonal distribution of gravity wave activity in Mars' lower atmosphere derived from MGS radio occultation data. *Geophys. Res. Let.* 2006, vol. 33, L01803. DOI: 10.1029/2005GL024037.

Fritts D.C. A review of gravity wave saturation processes, effects, and variability in the middle atmosphere. *Pure Appl. Geophys.* 1989, vol. 130, pp. 343–371.

Fritts D.C., Alexander M.J. Gravity wave dynamics and effects in the middle atmosphere. *Rev. Geophys.* 2003, vol. 41, no. 1, pp. 1–59. DOI: 10.1029/2001RG000106.

Gavrilov N.M., Karpova N.V., Jacobi Ch., Gavrilov A.N. Morphology of atmospheric refraction index variations at different altitudes from GPS/MET satellite observations. *J. Atmos. Sol.-Terr. Phys.* 2004, vol. 66, no. 6–9, pp. 427–435.

Gavrilov N.M., Manuilova R.O. Long-term global distributions of mesoscale variations in atmospheric radio refraction obtained from the GPS Champ Satellite Data. *Radiophysics and Quantum Electronics*. 2016, vol. 59, no. 7, pp. 535–545. DOI: 10.1007/s11141-016-9721-7.

Gill A.E. *Dinamika atmosfery i okeana* [Atmosphere-Ocean Dynamics]. Moscow: Mir Publ., 1986, vol. 1. 397 p. (In Russian). English edition: Gill A.E. *Atmosphere-Ocean Dynamics*. New York, London, Paris: Academic Press, 1982.

Gorbunov M.E., Gurvich A.S. Microlab-1 experiment: Multipath effects in the lower troposphere. *J. Geophys. Res.* 1998, vol.103, no. D12, pp. 13819–13826.

Gossard E.E, Hooke W.H. *Waves in the atmosphere.* Elsevier Scientific Publishing Co., Amsterdam-Oxford-New York, 1975.

Gubenko V.N., Andreev V.E., Pavelyev A.G. Detection of layering in the upper cloud layer of Venus northern polar atmosphere observed from radio occultation data. *J. Geophys. Res.* 2008a, vol. 113, E03001. DOI: 10.1029/2007JE002940.

Gubenko V.N., Pavelyev A.G., Andreev V.E. Determination of the intrinsic frequency and other wave parameters from a single vertical temperature or density profile measurement. *J. Geophys. Res.* 2008b, vol. 113, D08109. DOI: 10.1029/2007JD008920.

Gubenko V.N., Pavelyev A.G., Salimzyanov R.R., Pavelyev A.A. Reconstruction of internal gravity wave parameters from radio occultation retrievals of vertical temperature profiles in the Earth's atmosphere. *Atmos. Meas. Tech.* 2011, vol. 4, no. 10, pp. 2153–2162. DOI: 10.5194/amt-4-2153-2011.

Gubenko V.N., Pavelyev A.G., Salimzyanov R.R., Andreev V.E. A method for determination of internal gravity wave parameters from a vertical temperature or density profile measurement in the Earth's atmosphere. *Cosmic Res.* 2012, vol. 50, no. 1, pp. 21–31. DOI: 10.1134/S0010952512010029.

Gubenko V.N., Kirillovich I.A., Pavelyev A.G. Characteristics of internal waves in the Martian atmosphere obtained on the basis of an analysis of vertical temperature profiles of the Mars Global Surveyor mission. *Cosmic Res.* 2015, vol. 53, no. 2, pp. 133–142. DOI: 10.1134/S0010952515020021.

Gubenko V.N., Kirillovich I.A. Pavelyev A.G., Andreev V.E. Detection of saturated internal gravity waves and reconstruction of their characteristics in the Martian atmosphere. *Izvestiya vysshikh uchebnykh zavedenii. Fizika* [Russian Physics Journal]. 2016a, vol. 59, no. 12-2, pp. 46–49. (In Russian).

Gubenko V.N., Kirillovich I.A., Liou Y.-A., Pavelyev A.G. Monitoring of internal gravity waves in the Arctic and Antarctic atmosphere. *Izvestiya vysshikh uchebnykh zavedenii. Fizika* [Russian Physics Journal]. 2016b, vol. 59, no. 12-3, pp. 80–85. (In Russian).

Gubenko V.N., Pavelyev A.G., Andreev V.E., Kirillovich I.A., Salimzyanov R.R. Radio occultation investigations of internal waves and layered structures in atmospheres of the Earth, Mars and Venus. *Sovremennye Dostizheniya v Plazmennoi Geliogeofizike* [Modern Achievements in Plasma Heliogeophysics]. 2016c. Moscow: IKI RAN Publ., 2016c. pp. 548–554. (In Russian). URL: http://iki.cosmos.ru/books/2016petrukovich-2.pdf (accessed 31 March 2018).

Gubenko V.N., Pavelyev A.G., Kirillovich I.A., Liou Y.-A. Case study of inclined sporadic E layers in the Earth's ionosphere observed by CHAMP/GPS radio occultations: Coupling between the tilted plasma layers and internal waves. *Adv. Space Res.* 2018, vol. 61, iss. 7, pp. 1702–1716. DOI: 10.1016/j.asr.2017.10.001.

Hines C.O. Tropopausal mountain waves over Arecibo: A case study. *J. Atmos. Sci.* 1988, vol. 46, no. 4, pp. 476–488.

Horinouchi T., Tsuda T. Spatial structures and statistics of atmospheric gravity waves derived using a heuristic vertical

cross section extraction from COSMIC GPS radio occultation data. *J. Geophys. Res.* 2009, vol. 114, D16110. DOI: 10.1029/2008JD011068.

Liou Y.A., Pavelyev A.G., Huang C.Y., Igarashi K., Hocke K., Yan S.K. Analytic method for observation of the gravity waves using radio occultation data. *Geophys. Res. Let.* 2003, vol. 30, no. 20. CiteID 2021. DOI: 10.1029/2003GL017818.

Liou Y.A., Pavelyev A.G., Wickert J., Huang C.Y., Yan S.K., Liu S.F. Response of GPS occultation signals to atmospheric gravity waves and retrieval of gravity wave parameters. *GPS Solutions*. 2004, vol. 8, no. 2, pp. 103–111.

Noersomadi N., Tsuda T. Comparison of three retrievals of COSMIC GPS radio occultation results in the tropical upper troposphere and lower stratosphere. *Earth, Planets and Space*. 2017, vol. 69:125. DOI: 10.1186/s40623-017-0710-7.

Pavelyev A.G., Liou Y.A., Wickert J., Gubenko V.N., Pavelyev A.A., Matyugov S.S. New Applications and Advances of the GPS Radio Occultation Technology as Recovered by Analysis of the FORMOSAT-3/COSMIC and CHAMP Data-Base. *New Horizons in Occultation Research: Studies in Atmosphere and Climate*. Springer-Verlag, Berlin, Heidelberg. 2009, pp. 165–178. DOI: 10.1007/978-3-642-00321_9.

Pavelyev A.G., Liou Y.A., Zhang K., Wang C.S., Wickert J., Schmidt T., Gubenko V.N., Pavelyev A.A., Kuleshov Y. Identification and localization of layers in the ionosphere using the eikonal and amplitude of radio occultation signals. *Atmos. Meas. Tech*. 2012, vol. 5, no. 1, pp. 1–16. DOI: 10.5194/amt-5-1-2012.

Pavelyev A.G., Liou Y.A., Matyugov S.S., Pavelyev A.A., Gubenko V.N., Zhang K., Kuleshov Y. Application of the locality principle to radio occultation studies of the Earth's atmosphere and ionosphere. *Atmos. Meas. Tech*. 2015, vol. 8, no. 7, pp. 2885–2899. DOI: 10.5194/amt-8-2885-2015.

Peralta J., Sanchez-Lavega A., Lopez-Valverde M.A., Luz D., Machado P. Venus's major cloud feature as an equatorially trapped wave distorted by the wind. *Geophys. Res. Let*. 2015, vol. 42. DOI: 10.1002/2014GL062280.

Pfister L., Chan K.R., Bui T.P., Bowen S., Legg M., Gary B., Kelly K.; Proffitt M., Starr W. Gravity waves generated by a tropical cyclone during the STEP tropical field program: A case study. *J. Geophys. Res.* 1993, vol. 98, no. D5, pp. 8611–8638.

Rechou A., Kirkwood S., Arnault J., Dalin P. Short vertical-wavelength inertia gravity waves generated by a jet-front system at Arctic latitudes — VHF radar, radiosondes, and numerical modeling. *Atmos. Chem. Phys.* 2014, vol. 14, pp. 6785–6799. DOI: 10.5194/acp-14-6785-2014.

Sacha P., Foelsche U., Pisoft P. Analysis of internal gravity waves with GPS RO density profiles. *Atmos. Meas. Tech*. 2014, vol. 7, pp. 4123–4132. DOI: 10.5194/amt-7-4123-2014.

Steiner A.K., Kirchengast G. GW spectra from GPS/MET occultation observations. *J. Atmos. Ocean. Tech.* 2000, vol. 17, pp. 495–503.

Tsuda T., Hocke K. Vertical wave number spectrum of temperature fluctuations in the stratosphere using GPS occultation data. *J. Meteorol. Soc. Jpn.* 2002, vol. 80, no. 4B, pp. 1–13.

Tsuda T., Nishida M., Rocken C., Ware R.H. A global morphology of GW activity in the stratosphere revealed by the GPS occultation data (GPS/MET). *J. Geophys. Res*. 2000, vol. 105, no. D6, pp. 7257–7273.

Xiao C.Y., Hu X. Analysis on the global morphology of stratospheric gravity wave activity deduced from the COSMIC GPS occultation profiles. *GPS Solutions*. 2010, vol. 14, pp. 65–74. DOI: 10.1007/s10291-009-0146-z.

Zagar N., Jelic D., Blaauw M., Bechtold P. Energy spectra and inertia–gravity waves in global analyses. *J. Atmos. Sci.* 2017, vol. 74. no. 8, pp. 2447–2466. DOI: 10.1175/JAS-D-16-0341.1.

Zink F., Vincent R.A. Wavelet analysis of stratospheric gravity wave packets over Macquarie Island. 1. Wave parameters. *J. Geophys. Res.* 2001, vol. 106, no. D10, pp. 10275–10288.

http://www.sparc.sunysb.edu/

How to cite this article

Gubenko V.N., Kirillovich I.A. Diagnostics of internal atmospheric wave saturation and determination of their characteristics in Earth's stratosphere from radiosonde measurements. *Solar-Terrestrial Physics*. 2018. vol. 4, iss. 2. pp. 41–48. DOI: 10.12737/stp-42201807